

Complex Structural Imaging in the Tarakan Basin – A Case Study, Offshore Indonesia

J. Song, C. Reta-Tang, X. Ma, G. Rodriguez, B. Beck, N. Hokanson, J. Xu and A. Snyder, TGS

Summary

Increased industry exploration interest in the Tarakan Basin, offshore East Kalimantan, Indonesia, has stimulated a need for 3D seismic data that incorporates recent advances in imaging and velocity model building. The area forms part of an extensive Tertiary-age play fairway. New data is needed to assist in improving the understanding of the complex structural and stratigraphic setting of this important oil and gas province, particularly in prospect delineation and well planning. A reliable seismic image is crucial to understanding the complex fault system that dominates the regional structural framework in this area. In this paper we present a case history of some recent processing that resulted in high quality pre-stack depth migration (PSDM) seismic images from anisotropic VTI PSDM and a geologically-correlated velocity model.

Introduction

TGS' Tarakan Basin Bulungan 3D (TBB11) survey covers approximately 1793 km² over the southern part of the Bulungan sub-basin, East Kalimantan, Indonesia. It is adjacent to an earlier survey, the Tarakan Basin Nunukan 3D (TBN10), completed in mid-2011 and covering approximately 1625 km² (Figure 1) (Song, et al. 2011).

The processing objective of the TBB11 survey was to create, through tomographic velocity model refinement and high-resolution depth migration, high-quality images of structural and stratigraphic traps in a listric growth fault, deltaic/shelf depocenter setting. In this geologically complex area amplitude anomalies are found within the thin reservoirs and against and along the steeply dipping faults. In areas such as this, characterized by complex geology, strong lateral velocity variation and dipping structures, successful depth imaging depends on an accurate velocity model. The workflow adopted for this project utilized geologically-correlated VTI velocity model building and an application of high resolution tomography to update the velocity. This approach improved stratigraphic resolution, resulting in more accurate placement of events and better definition of faults, in what has traditionally been a poor data area.

Geological Setting and Structural Description of the Area

The Tarakan basin, typified by NNE–SSW normal faults developed in the marginal and offshore areas, is one of

several Tertiary rifted-margin sedimentary basins in eastern Borneo. As one of several sub-basins existing in the Tarakan basin, the Bulungan sub-basin is now situated at the mouth of the Bulungan River delta (Satyana et al., 1999).

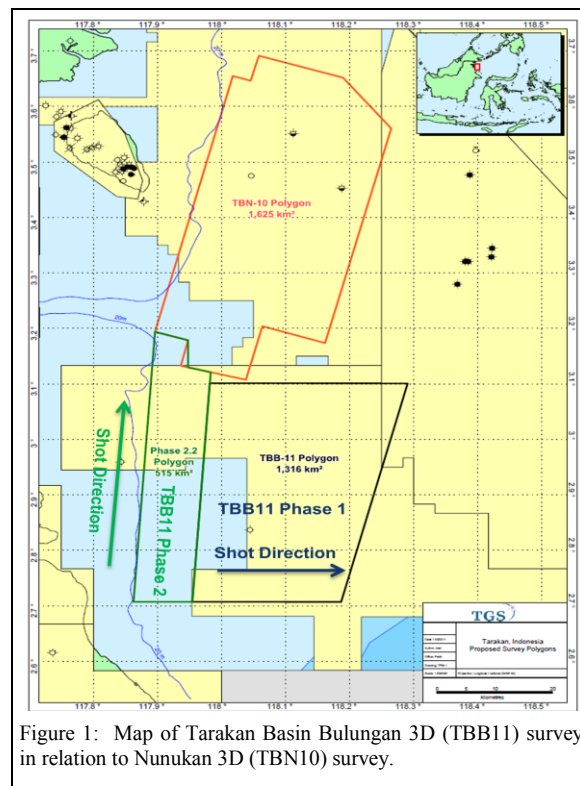


Figure 1: Map of Tarakan Basin Bulungan 3D (TBB11) survey in relation to Nunukan 3D (TBN10) survey.

In the Tarakan basin, the structural grain is dominated by NNE–SSW trending normal faults. These structures were formed on top of older NW–SE trending folds and are normal to the direction of the basin sedimentary thickening. Very gentle folds also play a role as hydrocarbon traps in association with stratigraphic entrapment. The prominent NW–SE anticlines, fragmented by NE–SW growth faults, have proved to be petroleum traps and have recently become primary targets for exploratory drilling.

Acquisition and Pre-Processing

The TBB11 survey was acquired in two phases, both with a bin size of 6.25 m x 25 m. The larger of the two phases (Phase 1) was acquired approximately East-West (shooting direction of 90.1°) and comprised 159 sail lines, totaling

Complex Structural Imaging In the Tarakan Basin

1311.3 square kilometers. Phase 2 was shot approximately North-South (shooting direction of 3.93°) and comprised 58 sail lines, totaling 494.4 square kilometers. The Phase 1 acquisition was completed May 14, 2011 and the Phase 2 acquisition was completed June 2, 2011. The project location is shown in Figure 1.

During preprocessing, special effort was spent in the attenuation of residual multiple, in particular pegleg multiples that affect the target level. Moreover, the data is also affected by residual interbed multiples. The major demultiple steps included 3D SRME, High Resolution Radon De-Multiple, and Shallow Water De-Multiple (SWD) (applied where the water depth is less than 300 ms).

Even after the complete de-multiple sequence had been applied, surface-related multiples and interbed multiples continued to pose a challenge, especially in the shallow to mid-section. The remaining multiple energy was attenuated using the SMELT technique (Stepwise Multiple Elimination using Linear Transforms) described by Hardwick, et al., (2010). The SMELT “multiple model” is gradually built up by a series of linear transforms in the CMP domain after flattening multiples with a constant normal moveout correction (NMO) in steps between water velocity and maximum pegleg velocity. It applies a narrow forward-inverse Tau-P transform with the P-range determined by the velocity step and constant NMO velocity value. The outputs are primaries, surface-related multiples and internal multiples associated with that velocity step. A selectively windowed subtraction is then employed to subtract the multiple energy from the input CDP gather. As multiples are flattened prior to transformation the process is unaffected by aliasing. SMELT was only applied in the deeper water areas and targeted the near-to-middle offsets where most of the remaining multiples existed at this stage.

The decision was made to use the Phase 1 acquisition geometry for the processing of both Phase 1 and 2. The difference in shooting direction between the two phases is approximately 84 degrees. A straightforward regridding of the Phase 2 onto the Phase 1 grid generates issues of spatial aliasing and incomplete fold coverage in both midpoint and offset domains, which in turn creates Kirchhoff migration artifacts. To overcome these problems offset regularization was performed on the Phase 2 data after regridding to the Phase 1 geometry. Offset regularization was done by an inversion method in the frequency F-kx-ky domain (see Duijndam, et al, (1995) and Cai, et al, (2009)). The windowed input traces are transformed from the time-x-y domain to the frequency F-kx-ky domain by the non-uniform Fourier transform. Arbitrary traces can be interpolated by applying an inverse FFT to the spectrum. An inversion process is applied to reduce spectrum leakage

by matching the spectra of interpolated traces and input traces.

Tomography Velocity Update and PSDM VTI Migration

The initial velocity model for input to tomography was adapted from the PSTM velocity model. The PSTM model was first converted into the depth domain and embedded with the water velocity to generate the initial PSDM velocity. The water velocity was determined using CDP gathers from both shallow and deep water areas. After thorough testing, a velocity of 1525 m/s was found to be optimum for this area. The model was then smoothed with a depth-varying smoother with heavier smoothing down deep.

Four grid tomography iterations were performed during the velocity analysis. Each tomography iteration was followed by a new depth Kirchhoff pre-stack VTI migration after the tomography velocity update was applied. New migrated gathers feed the next tomography as input. For each tomography iteration residual curvature of the gathers is determined through event scanning. These curvatures along with the dip fields derived from the migrated stacks are input into the tomography ray tracing step. The output of the tomographic inversion is a velocity perturbation cube, which is added to the previously used depth migration velocity model.

During the first iteration of tomography short period velocity variations in the shallow water area were modeled by a pass of ultra high resolution tomography. The isotropic migration in this iteration outputs data with a 5 m depth step, 100 m offset increment and 60-fold gathers. Tomography is performed on a 75 by 75 m grid with a 25 m depth increment and is constrained to the region from the waterbottom to 4 km depth.

One checkshot was available for this survey for velocity calibration and VTI anisotropic parameter estimation. The velocity model at the checkshot location was calibrated with the checkshot velocity. After calibration, the derived scalar was extrapolated along the waterbottom and other horizons interpreted from the migration stack volume. The anisotropic parameters delta and epsilon were then derived using focusing analysis (FAN) around the checkshot location. FAN involves constructing the true focusing operator by demigration of a CIG back to the time domain, then calculating the focusing operator for different values of epsilon and delta from the focal point (zero offset image), and then searching for the minimum objective function (the difference between the true focusing operator and the calculated focusing operators) (Cai, et al., 2009).

Complex Structural Imaging In the Tarakan Basin

The next two passes of tomography were carried out using a 200 m by 200 m grid and a depth increment of 50 m to globally update the velocity model. These coarser grid tomography iterations are intended to focus on large residual moveout and regional velocity errors. To further refine the velocities, especially in the fault zones and areas having detailed structure, the last pass of tomography was run on a fine grid of 100 x 100 x 50 m. After each iteration a careful check on the match between interval velocity functions extracted from the model and the checkshot at the well location is conducted. The final velocity model is shown in Figure 2.

The final VTI Kirchhoff pre-stack depth migration was run to produce 60-fold output, with a 25 by 25 m output bin size, 100 m offset increment and 5 m depth step.

Results

Results from the final Kirchhoff pre-stack depth migration are shown in (Figures 3a-c). A number of structural features such as fault definition, coherency and geologic sensibility of the events can be seen. These are due to the resolution of the final velocity model and depth migration's ability to handle lateral velocity variations. The colors in the background represent the final velocity field. Note how the lateral velocity changes conform to the fault blocks and the velocity increases across the top basement reflector, which makes sense geologically. Also, normal fault structures are clearly imaged (Figure 3b).

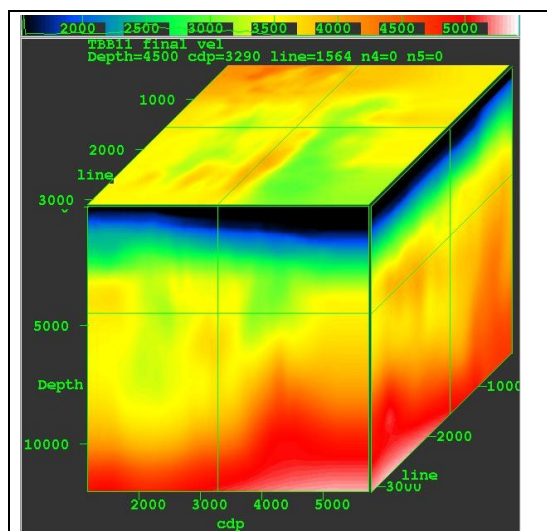


Figure 2: Final velocity model

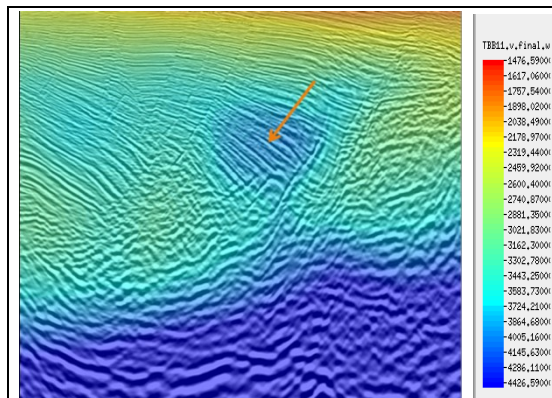


Figure 3a: Dipping reflector unconformable with flat reflector

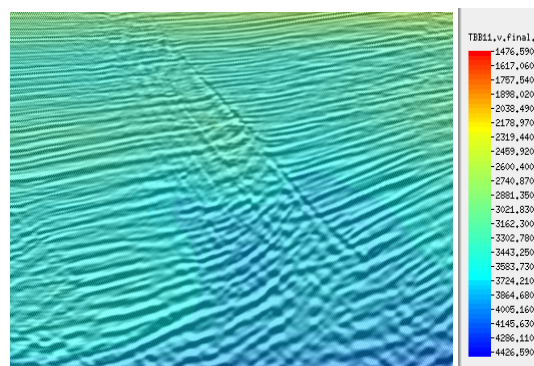


Figure 3b: Normal fault structure

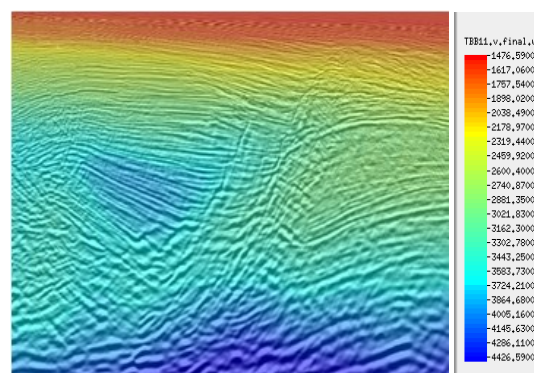


Figure 3c: The lateral velocity changes conform to the fault blocks

The high-resolution tomography resulted in the accurate imaging of numerous structural details, including a variety of dipping reflectors in the middle and shallow zones

Complex Structural Imaging In the Tarakan Basin

(Figures 3a and 3c); a strong, dipping reflector that is unconformable with the other reflectors (Figure 3a); and the numerous flat-lying reflectors (Figures 3b-c).

A sharp vertical change in velocity can be observed (Figure 3a), in which the velocity rises rapidly from 3500 m/s to 4500 m/s. This abrupt change may indicate the geologically sharp unconformity at the base of the Paleogene, Neogene and Quaternary sediments.

Comparing the pre-stack depth migration image with the pre-stack time migration image in the middle and deep parts, depth imaging gives more continuous events and interpretable structures, especially in the fault zones (Figure 4).

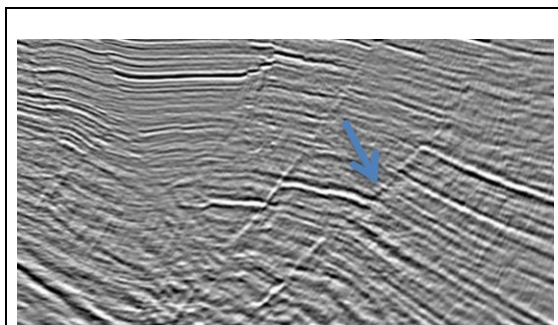


Figure 4a: Pre-stack time migration

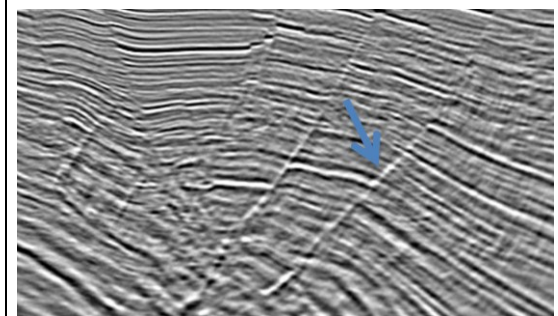


Figure 4b: Pre-stack depth migration

Conclusion

High resolution tomography and Kirchhoff pre-stack depth migration improved the seismic imaging and achieved better focusing and positioning of the structures and better continuity of the reflectors, fault plane resolution and depth matching with respect to well ties. The derived depth volumes provide strong support for well planning. The velocity model estimated by grid tomography is very detailed and accurate, which allows more precise picking of

the reservoirs, giving interpreters a better tool to further understand the area's petroleum system.

In addition, the dipping nature of some events was ascertained on the seismic images and some distinguishable horizons lying immediately over the base sediment unconformity were imaged. Some visible bright spots in the medium depth range, well-imaged, may indicate the presence of gas.

Acknowledgments

The authors would like to thank the management of TGS for their permission to publish the data. We would also like to thank Landis Newbanks and Steve Smith for their excellent QC support, and Zhiming Li, Terry Hart and Kenny Lambert for their support throughout the life of the project. The authors also thank Simon Baldock, Laurie Geiger and Chuck Mason for proof reading.

EDITED REFERENCES

Note: This reference list is a copy-edited version of the reference list submitted by the author. Reference lists for the 2012 SEG Technical Program Expanded Abstracts have been copy edited so that references provided with the online metadata for each paper will achieve a high degree of linking to cited sources that appear on the Web.

REFERENCES

- Cai, J., Y. He, Z. Li, B. Wang, and M. Guo, 2009, TTI/VTI anisotropy estimation by focusing analysis, Part I: Theory: 79th Annual International Meeting, SEG, Expanded Abstracts, 301–305.
- Cai, J., S. Dong, M. Guo, S. Sen, J. Ji, B. Wang, and Z. Li, 2009, Some aspects on data interpolation: Multiple prediction and imaging: 79th Annual International Meeting, SEG, Expanded Abstracts, 3178–3182.
- Duijndam, A., J. Schils, and M. A. Schonewille, 1995, Reconstruction of bandlimited, irregularly-sampled signals: 65th Annual International Meeting, SEG, Expanded Abstracts, 1350–1353.
- Hardwick, A., C. Lang, and B. Kjøllhamar, 2010, Stepwise multiple elimination using linear transforms: An alternative approach to SRME for stacking multiple-free near offsets in the Barents Sea: 80th Annual International Meeting, SEG, Expanded Abstracts, 3426–3430.
- Satyana, A., D. Nugroho, and I. Surantoko, 1999, Tectonic controls on the hydrocarbon habitats of the Barito, Kutei, and Tarakan Basins, eastern Kalimantan, Indonesia: Major dissimilarities in adjoining basins: *Journal of Asian Earth Sciences*, **17**, no. 1-2, 99–122.
- Song, J., C. Retã-Tang, X. Ma, J. Wilhite, and Laurie Geiger, 2011, Improved 3D seismic imaging through depth migration and tomography: An Indonesia case study: *PESA News Resources*, **115**, 50–52.